



저작자표시-비영리-변경금지 2.0 대한민국

이용자는 아래의 조건을 따르는 경우에 한하여 자유롭게

- 이 저작물을 복제, 배포, 전송, 전시, 공연 및 방송할 수 있습니다.

다음과 같은 조건을 따라야 합니다:



저작자표시. 귀하는 원저작자를 표시하여야 합니다.



비영리. 귀하는 이 저작물을 영리 목적으로 이용할 수 없습니다.



변경금지. 귀하는 이 저작물을 개작, 변형 또는 가공할 수 없습니다.

- 귀하는, 이 저작물의 재이용이나 배포의 경우, 이 저작물에 적용된 이용허락조건을 명확하게 나타내어야 합니다.
- 저작권자로부터 별도의 허가를 받으면 이러한 조건들은 적용되지 않습니다.

저작권법에 따른 이용자의 권리는 위의 내용에 의하여 영향을 받지 않습니다.

이것은 [이용허락규약\(Legal Code\)](#)을 이해하기 쉽게 요약한 것입니다.

[Disclaimer](#)

Development of novel cancer therapies through overcoming of anti-apoptotic mechanism of lung cancer observed during ionizing radiation therapy

Jung Mo Lee

Department of Medicine

The Graduate School, Yonsei University

Development of novel cancer therapies through overcoming of anti-apoptotic mechanism of lung cancer observed during ionizing radiation therapy

Jung Mo Lee

Department of Medicine

The Graduate School, Yonsei University

Development of novel cancer therapies through overcoming of anti-apoptotic mechanism of lung cancer observed during ionizing radiation therapy

Directed by Professor Yoon Soo Chang

The Doctoral Dissertation
submitted to the Department of Medicine,
the Graduate School of Yonsei University
in partial fulfillment of the requirements for the degree of
Doctor of Philosophy

Jung Mo Lee

December 2021

This certifies that the Doctoral Dissertation
of Jung Mo Lee is approved.

Thesis Supervisor : Yoon Soo Chang

Thesis Committee Member#1 : Eun Young Kim

Thesis Committee Member#2 : Jin Gu Lee

Thesis Committee Member#3: Jaeho Cho

Thesis Committee Member#4: Seung Hun Jang

The Graduate School
Yonsei University
December 2021

ACKNOWLEDGEMENTS

First of all, I want to express my sincere gratitude to Professor Yoon Soo Chang for his supervision on this whole study. I admire his passionate belief in lung cancer research.

I am incredibly grateful to Professor Eun Young Kim, who guided and supported this study overall. This study could not have been conducted without her guidance.

In addition, I am profoundly thankful to Professor Jin Gu Lee, Jaeho Cho, and Seung Hun Jang, who led the academic discussion and gave keen advice on this study. Their specialist assistance was significant and crucial in this study.

Finally, I wish to send my appreciation and boundless love to my parents, parents-in-law, wife, and two of my adorable kids. They always give me unlimited support and love.

<TABLE OF CONTENTS>

ABSTRACT	1
I. INTRODUCTION	3
II. MATERIALS AND METHODS	6
1. Cell lines, chemicals, and antibodies	6
2. Cell irradiation immunoblotting	6
3. Immunofluorescence (IF)	6
4. Clonogenic assay	7
5. Reverse transcription polymerase chain reaction (RT-PCR)	7
6. Mouse irradiation and imaging	7
7. Immunohistochemistry (IHC)	8
8. Statistical analysis	9
9. Ethical approval and consent to participate	9
III. RESULTS	10
1. Irradiation treatment increased the expression of antiapoptotic proteins in A549 and H460 cells	10
2. Upregulation of Bcl-2 family proteins was caused by irradiation-mediated signal transducer and activator of transcription (STAT) 3 activation and induction of the autophagic pathway	14
3. ABT-737 enhanced the radiosensitivity of A549 and H460 cells	19
4. The combination of ABT-737 and irradiation showed increased antitumor efficacy in the Kras ^{G12D} :p53 ^{fl/fl} lung cancer mouse model	21
IV. DISCUSSION	26
V. CONCLUSION	29
REFERENCES	30
ABSTRACT(IN KOREAN)	34

LIST OF FIGURES

Figure 1. Irradiation treatment increased the expression of antiapoptotic proteins in A549 and H460 cells	11
Figure 2. Upregulation of Bcl-2 family proteins was caused by irradiation-mediated STAT3 activation and induction of the autophagic pathway	16
Figure 3. ABT-737 enhanced the radiosensitivity of A549 and H460 cells	20
Figure 4. The combination of ABT-737 and irradiation increased antitumor efficacy in a Kras ^{G12D} :p53 ^{fl/fl} lung cancer mouse model	22

ABSTRACT

Development of novel cancer therapies through overcoming of anti-apoptotic mechanism of lung cancer observed during ionizing radiation therapy

Jung Mo Lee

*Department of Medicine
The Graduate School, Yonsei University*

(Directed by Professor Yoon Soo Chang)

Tumor radioresistance and dose-limiting toxicity restrict the curative potential of radiotherapy, requiring novel approaches to overcome the limitations and augment the efficacy. Here, we investigated the effects of signal transducer and activator of transcription 3 (STAT3) activation and autophagy induction by irradiation on antiapoptotic proteins and the effectiveness of the BH3 mimetic ABT-737 as a radiosensitizer using K-ras mutant non-small cell lung cancer (NSCLC) cells and a Kras^{G12D}:p53^{fl/fl} mouse (KP mouse) model.

A549 and H460 cells were irradiated, and the expression of Bcl-2 family proteins, the JAK/STAT transcriptional pathway, and the autophagic pathway were evaluated by immunoblotting. The radiosensitizing effects of ABT-737 were evaluated using A549 and H460 cell lines with clonogenic assays and using a KP mouse model with microcomputed tomography and immunohistochemistry.

In A549 and H460 cells and mouse lung tissue, irradiation-induced overexpression of the antiapoptotic molecules Bcl-xL, Bcl-2, Bcl-w, and Mcl-1 through the JAK/STAT transcriptional signaling induced dysfunction of the

autophagic pathway. After treatment with ABT-737 and exposure to irradiation, the number of surviving clones in the cotreatment group was significantly lower than that in the group treated with radiation or ABT-737 alone. In the KP mouse lung cancer model, cotreatment with ABT-737 and radiation induced significant tumor regression; however, body weight changes in the combination group were not significantly different, suggesting that combination treatment did not cause systemic toxicity.

These findings supported the radiosensitizing activity of ABT-737 in preclinical models and suggested that clinical trials using this strategy may be beneficial in K-ras mutant NSCLC.

Key words : non-small cell lung cancer, apoptosis, radiation sensitizer, ABT-737

Development of novel cancer therapies through overcoming of anti-apoptotic mechanism of lung cancer observed during ionizing radiation therapy

Jung Mo Lee

*Department of Medicine
The Graduate School, Yonsei University*

(Directed by Professor Yoon Soo Chang)

I. INTRODUCTION

Lung cancer is a leading cause of cancer mortality worldwide. The American Cancer Society estimated that 235,760 new cases of lung cancer will occur and that 131,880 patients will die of this devastating disease in the United States of America in 2021.¹ In recent years, there has been increasing awareness of the molecular pathways that drive malignancy, particularly in lung adenocarcinoma, and the development of agents that target these pathways. Although the availability of new systemic therapeutic agents represents substantial progression, these agents are not sufficiently efficacious.² Moreover, the median and 5-year survival rates for patients with all stages of non-small cell lung cancer (NSCLC) and small cell lung cancer are poor, and compared with the progress made for other types of cancers, improvements in survival in recent years have been marginal at best.

Radiotherapy is one of the main treatment modalities in lung cancer and has an important role in all stages of lung cancer, as either definitive or palliative therapy.

However, tumor radioresistance and dose-limiting toxicity restrict the curative potential of radiotherapy.^{3,4} Therefore, novel approaches are needed to overcome these limitations and to augment the effects of radiation. Ionizing radiation provokes the activation of signal transducer and activator of transcription 3 (STAT3), which contributes to the development of radiation resistance through various mechanisms, including the upregulation of antiapoptotic genes, the alteration of the cell cycle, the promotion of proliferation, and the induction of epithelial to mesenchymal transition.⁵ Aberrations in the apoptotic pathway after irradiation can attenuate the therapeutic effects of radiation. Therefore, manipulation of radiation-induced apoptosis is one strategy to overcome radioresistance in NSCLC.

Apoptosis involves a cascade of caspase proteases released from the mitochondria and regulated by Bcl-2 proteins. The Bcl-2 family is comprised of antiapoptotic members, such as Bcl-2, Mcl-1, and Bcl-xL, and proapoptotic members, such as Bax, Bak, and Bid.⁶ The balance between cell survival and cell death is modulated by the ratios and interactions of antiapoptotic and proapoptotic Bcl-2 family proteins.⁷ Defects in the apoptotic pathway correlate with cellular resistance to therapy and are frequently observed in NSCLC.^{8,9} Moreover, overexpression of Bcl-2 or Bcl-xL is observed in several cancers, and elevated expression of Bcl-2, Mcl-1, and Bcl-xL is related to resistance to radiation-induced apoptosis.^{10,11}

BH3 mimetics show a biochemical affinity for specific anti-apoptotic BCL-2 proteins, which is linked to their ability to kill specific cells.^{12,13} ABT-737, a 'first-in-class' BH3 mimetic, is a small molecule inhibitor that binds with high affinity to Bcl-xL, Bcl-2 and Bcl-w, inducing the mitochondrial pathway of apoptosis that begins with the permeabilization of the mitochondrial outer membrane. Some studies have shown that ABT-737 can enhance the radiosensitivity of various solid cancers. However, to the best of our knowledge, the radiosensitizing effect of ABT-737 has not yet been studied in NSCLC.

In this study, we hypothesized that the inhibition of Bcl-2 might enhance the tumoricidal effects of radiation in lung cancer. Therefore, we explored an approach to overcome radiation resistance by targeting antiapoptotic Bcl-2 family proteins using a combination of ABT-737 with radiation in K-ras mutant NSCLC cell lines and a lung cancer-induced LSL *K-ras* G12D and p53^{fl/fl} mouse model.

II. MATERIALS AND METHODS

1. Cell lines, chemicals, and antibodies.

A549 and H460 cells were purchased from ATCC (Manassas, VA, USA) in 2012. ABT-737 was obtained from AdooQ Bioscience (Irvine, CA, USA), and its chemical and crystal structures are described elsewhere.^{14,15} Antibodies, unless otherwise stated, were obtained from Cell Signaling Technology (Danvers, MA, USA).

2. Cell irradiation immunoblotting.

A549 and H460 lung cancer cells were irradiated at doses specified in each experiment up to 6 Gy using an X-rad 320 irradiator (Precision X-Ray, North Branford, CT, USA). Cells were harvested on ice using 2× Laemmli sample buffer containing protease and phosphatase inhibitors (Sigma–Aldrich, St. Louis, MO, USA). After sonication, 30–50 mg of lysate was separated by gel electrophoresis on 7.5–12% polyacrylamide gels and transferred onto nitrocellulose membranes (Bio–Rad Laboratories, Inc., Richmond, CA, USA). The expression level of each protein was measured using ImageJ (NIH, Bethesda, MD, USA) and quantified relative to that of β -actin.

3. Immunofluorescence (IF).

A549 and H460 lung cancer cells were irradiated with a dose of 4 Gy. After irradiation, the cells were incubated at 37 °C in a humidified atmosphere containing 5% CO₂/95% air for 24 h. After incubation, the cells were fixed and permeabilized with cold 100% MeOH and subsequently incubated overnight with primary antibodies against Bcl-xL, LC3A/B, and p62 in antibody diluent at a 1:100 dilution. After this step, the cells were subsequently incubated for 90 min with secondary antibodies against Alexa Fluor 488 and Alexa Fluor 555 in antibody diluent at a 1:1000 dilution, followed by incubation

with DAPI in phosphate-buffered saline (PBS) for DNA staining for 1 min. Images were taken using a confocal microscope (Zeiss; LSM780). All experiments were replicated three times. The corrected total cell fluorescence (CTCF) was measured using ImageJ.

4. Clonogenic assay.

A549 and H460 lung cancer cells were treated with 0.1% dimethylsulfoxide (DMSO) or 1 μ M ABT-737 and then irradiated with a dose of 2 Gy. After irradiation, the cells were incubated at 37 °C in a humidified atmosphere containing 5% CO₂/95% air for 10–14 days. After incubation, the cells were rinsed with PBS and stained for 30 min with a mixture of 6.0% glutaraldehyde and 0.5% crystal violet.¹⁶ After staining, colonies were counted using a cutoff of 50 viable cells. Experiments were conducted in triplicate, and means, standard deviations, and *p* values were calculated using Student's *t*-tests.

5. Reverse transcription polymerase chain reaction (RT–PCR).

A549 and H460 cells were irradiated with a dose of 2 Gy. After irradiation, total RNA was extracted using TRI reagent (Ambion, Austin, TX, USA). Quantitative reverse transcription polymerase chain reaction (RT–PCR) analysis was performed using TaqMan gene expression assay reagents (Thermo Fisher Scientific, Waltham, MA, USA) and a StepOnePlus RT-PCR system (Applied Biosystems, Carlsbad, CA, USA) using an inventoried primer-probe set. Three independent experiments were conducted.

6. Mouse irradiation and imaging.

LSL *K-ras* G12D and p53^{fl/fl} mice were obtained from the NCI mouse repository (<http://mouse.ncifcrf.gov/>), bred, and genotyped according to the supplier's guidelines. AdCre virus was obtained from the Gene Transfer Vector Core of the University of Iowa (Iowa City, IA, USA). LSL *K-ras* G12D and p53^{fl/fl} mice inhaled 5×10^7 PFU

AdCre virus at 8 weeks after birth. Then, 12 ± 2 weeks after AdCre particle inhalation, the mice were randomized and treated with either vehicle or ABT-737 (50 mg/kg, intraperitoneal injection, daily) for 3 days. The mice underwent microcomputed tomography (micro-CT) using a small animal eXplore Locus micro-CT (GE Healthcare, Little Chalfont, UK) under isoflurane anesthesia (45 μ m resolution, 80 kV, 450 μ A current) and were irradiated in the left lung with 10 Gy using an X-rad 320 irradiator (Precision X-Ray, North Branford, CT, USA). After 2 weeks, the second round of micro-CT was performed to determine the therapeutic effects, and lungs were harvested for histological analysis.

Treatment response was evaluated by CT image analysis. We detect all measurable tumors on CT images. To measure changes in tumor size, the longest diameter of the tumor on each side of the lung was quantified using Adobe Photoshop (Adobe Systems, San Jose, CA, USA). Changes in tumor size (%) were calculated as follows: $(\text{diameter}_{\text{before}} - \text{diameter}_{\text{after}}) / \text{diameter}_{\text{before}} \times 100$ for each side of the lung.

7. Immunohistochemistry (IHC).

Mice were sacrificed after the second micro-CT, and the expression of activated caspase-3 was analyzed by immunohistochemistry (IHC) using the LABS2 System (Dako, Carpinteria, CA, USA) according to the manufacturer's instructions. Briefly, sections were deparaffinized, rehydrated, immersed in 3% H₂O₂ in methanol solution, and then, they were incubated overnight with primary antibodies against activated caspase-3 in antibody diluent (Dako) at a 1:100 dilution. Sections were incubated for 10 min with biotinylated linker and processed using avidin/biotin IHC techniques. 3,3'-Diaminobenzidine (DAB) was used as a chromogen in conjunction with the Liquid DAB Substrate kit (Novacastra, Newcastle, UK). The number of apoptotic bodies per high-power field (400 \times) was counted in five fields, and the mean numbers

were compared using Student's *t*-tests. Protein expression was measured and quantified using ImageJ.

8. Statistical analysis.

Independent sample *t*-tests were used for univariate analysis of continuous variables. Differences in tumor area changes among groups were analyzed by Mann–Whitney U tests. Predictive factors for overall survival were calculated using the Kaplan–Meier estimate. SPSS software (v. 23; SPSS, Chicago, IL, USA) was used for statistical analysis. All statistical analyses were two-tailed, and *p* values of less than 0.05 were interpreted to indicate statistical significance.

9. Ethical approval and consent to participate.

This animal study was approved by the Institutional Animal Care and Use Committee of the Department of Laboratory Animal Resources, Yonsei Biomedical Research Institute, Yonsei University College of Medicine (2015-0307), following the guidelines of the American Association for the Assessment and Accreditation of Laboratory Animal Care.

III. RESULTS

1. Irradiation treatment increased the expression of antiapoptotic proteins in A549 and H460 cells

Overexpression of Bcl-2 family antiapoptotic proteins is associated with resistance to radiotherapy. To identify antiapoptotic molecules influenced by irradiation, A549 and H460 cells were irradiated, and the expression of antiapoptotic proteins of the Bcl-2 family was evaluated by immunoblotting at 24 and 48 h after irradiation. At 24 h after irradiation, the expression levels of Bcl-xL, Bcl-w, Mcl-1, and γ -H2AX increased as the dose of radiation increased. Similar results were obtained at 48 h after irradiation, but this change was more pronounced after 24 h (Fig. 1A and 1B). To determine the effects of irradiation in vivo, LSL K-ras G12D and p53^{fl/fl} mice were irradiated in the left lung with 10 Gy. (Fig. 1C) To evaluate the effects of radiation therapy on the same subject, only the left lung of the mouse was treated with radiation, and irradiated lung (Lt) and nonirradiated lung (Rt) were compared. The first mouse was sacrificed, the lungs were harvested 4 hours after irradiation, and the second mouse was sacrificed 24 hours after radiation treatment. The expression of antiapoptotic proteins was evaluated by immunoblotting using lung tissue lysates at 4 and 24 h after irradiation. Similar to the results in A549 and H460 cells, the expression levels of Bcl-xL, Bcl-2, Bcl-w, and Mcl-1 were increased in the irradiated lungs at 4 and 24 h after irradiation (Fig. 1D). Confocal microscopy revealed an increase in Bcl-xL expression as a response of A549 and H460 cells to 4 Gy of radiation. The expression of Bcl-xL (CTCF) was increased after 4 Gy of irradiation in both cell lines ($p < 0.05$) (Fig. 1E). Additionally, we performed IHC analysis of Bcl-xL. The percentage of Bcl-xL-positive cells was calculated by randomly selecting 5 different sites. A total of 28.14% of cells in the control lung (right lung) and 57.45% of cells in the irradiated lung (left lung) were

positive for Bcl-xL ($p < 0.001$), indicating that radiation augmented a subset of antiapoptotic molecules (Fig. 1F).

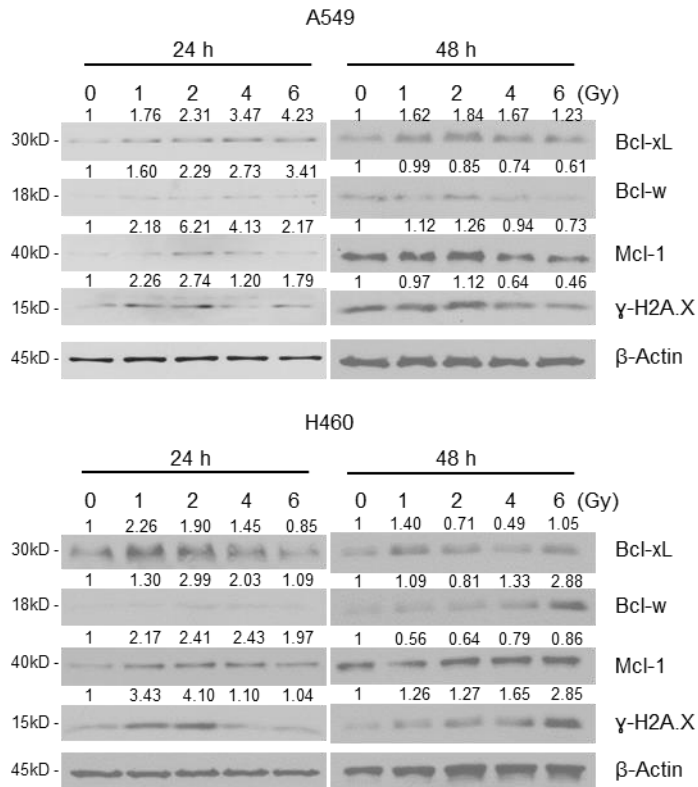


Figure 1A, 1B. A549 and H460 cells were irradiated, and the expression of antiapoptotic members of the Bcl-2 protein family was evaluated by immunoblotting 24 and 48 hours after irradiation.

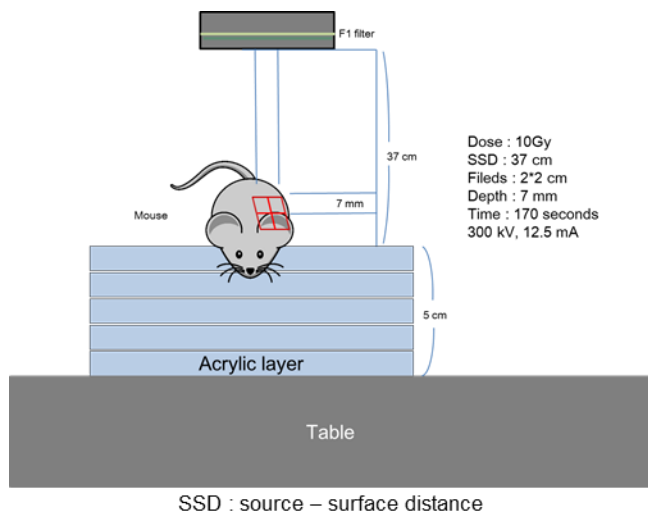


Figure 1C. Schematic depiction of the radiation protocol.

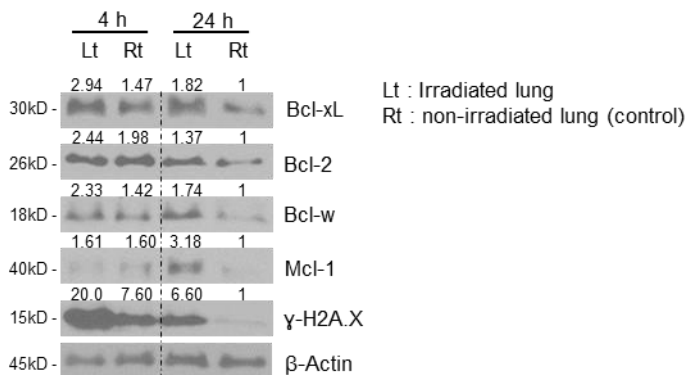


Figure 1D. LSL *K-ras* G12D and p53^{fl/fl} mice were irradiated only in the left lung, and the irradiated lung (Lt) and nonirradiated lung (Rt) were compared. The expression of antiapoptotic members of the Bcl-2 protein family was evaluated by immunoblotting using lysates from left and right lung tissues.

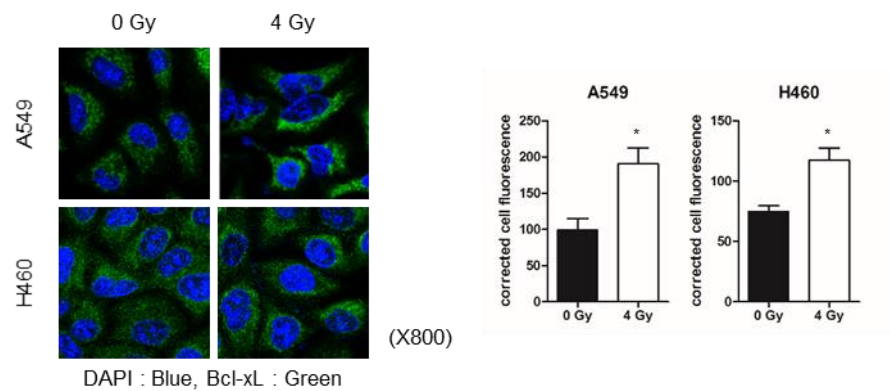


Figure 1E. Confocal microscopy images of A549 and H460 cells after immunofluorescence for Bcl-xL (green) protein at 24 hours after irradiation (magnification: 800 \times). Asterisks indicate significant differences to control; * $p < 0.05$.

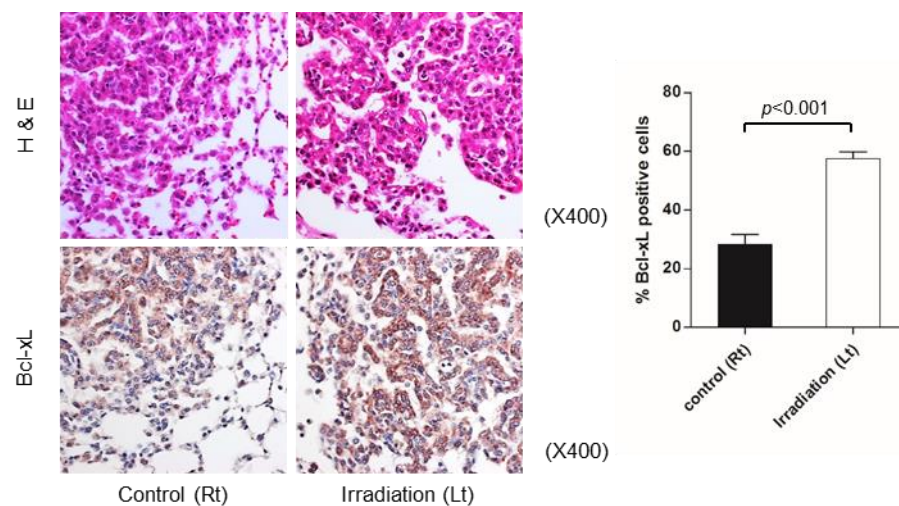


Figure 1F. H&E staining and Bcl-xL immunohistochemical analysis of both lungs of the mice. For immunohistochemistry, DAB was used as a chromogen (magnification: 400 \times). Group averages are graphed, and error bars represent the S.E.M.

2. Upregulation of Bcl-2 family proteins was caused by irradiation-mediated signal transducer and activator of transcription (STAT) 3 activation and induction of the autophagic pathway

To evaluate changes in the expression of antiapoptotic molecules at the transcriptional level after irradiation, A549 and H460 cells were irradiated, and real-time PCR was used to quantify the mRNA expression of antiapoptotic molecules. The mRNA expression levels of Bcl-w and Bcl-xL were increased in A549 cells; the increase in Bcl-w mRNA was more prominent than those of the other molecules (Fig. 2A). Bcl-2 mRNA was not detected in A549 cells, consistent with known reference data (<http://www.proteinatlas.org/ENSG00000171791-BCL2/cell/CAB000003>). In H460 cells, only the Bcl-2 mRNA level rose, and there was no clear increase in the mRNA expression of other molecules at 6 and 24 h after irradiation (Fig. 2A). Taken together, these findings did not adequately explain why irradiation induced overexpression of antiapoptotic members of the Bcl-2 protein family at the transcriptional level; another mechanism or mixed mechanism was expected to modulate protein expression.

Therefore, we next tested whether the augmented expression of the antiapoptotic protein was mediated by STAT3 activation. To this end, we evaluated the levels of phosphorylated Src, Janus kinase (JAK) 2, and STAT3 by immunoblotting after 1 Gy irradiation in A549 and H460 cells. The expression of p-Src, p-JAK2 and p-STAT3 was increased after irradiation in H460 cells. In A549 cells, the levels of phosphorylated JAK2 were increased after irradiation, and phosphorylated Src and STAT3 peaked at 2 h after irradiation and then decreased with the passage of time. These findings suggested that the phosphorylation of Src was related to the phosphorylation of STAT3 through JAK2 over time (Fig. 2B). To confirm the effects of radiation on the expression of Bcl-xL by irradiation-mediated activation of the Src pathway, additional experiments were performed using the Src inhibitor dasatinib (Fig. 2C). A549 and H460 cells were exposed to 1 Gy radiation and/or 50 nM dasatinib for 2 h. Levels of phospho (p)-Src,

p-JAK2, p-STAT3, and p-H2AX (Ser139) were evaluated by immunoblotting at 2 h after treatment. Pretreatment with dasatinib suppressed the elevation of p-STAT3 by irradiation in both cell lines.

Additionally, to identify the effects of posttranscriptional modification of antiapoptotic members of the Bcl-2 protein, we also examined changes in proteins associated with irradiation and autophagy. The expression levels of LC3A/B, p62, and Atg7 were evaluated by immunoblotting at 24 h after 2 Gy of irradiation. In A549 cells, the expression of LC3A/B, mainly the expression of the 14 kD band LC3A/B-II, increased with a rise in the radiation dose. The expression of LC3A/B-II approached a peak at 4 Gy of radiation and then gradually diminished. The expression of ATG7 approached a maximum at 2 Gy of radiation and steadily declined. p62 expression was partially augmented after 1 Gy of radiation and decreased with an increase in the radiation dose. In H460 cells, the expression of LC3A/B and LC3A/B-II approached a peak at 2 Gy of radiation and then gradually diminished. The expression of ATG7 was augmented in the radiation groups compared with the control group, although dose-specific changes were not constant. The expression of p62 increased partially after 1 Gy of radiation and was reduced with increasing doses of radiation (Fig. 2D). In immunofluorescence staining of A549 and H460 cells after 4 Gy of radiation, the expression of LC3A/B and p62 (CTCF) was increased after 4 Gy of irradiation in both cell lines ($p < 0.05$) (Fig. 2E). To confirm the effects of radiation on the expression of antiapoptotic proteins by irradiation-mediated activation of autophagy, additional experiments were performed using the autophagy inhibitor wortmannin (Fig. 2F). A549 and H460 cells were exposed to 2 Gy of radiation and/or 2.5 μ M wortmannin for 24 hours. The levels of LC3A/B, Atg 7, p62, p-H2AX (Ser139), and antiapoptotic proteins were evaluated by immunoblotting 24 hours after treatment. In A549 and H460 cells, the expression of LC3A/B-II increased after irradiation but decreased when the cells were treated with radiation and wortmannin. The expression of ATG7 was also increased after irradiation and decreased when treated with wortmannin and radiation together. The expression of

p62 diminished after 2 Gy of radiation but increased slightly when the cells were treated with radiation and wortmannin. The expression of the antiapoptotic proteins Bcl-xL and Bcl-w was augmented after 2 Gy of radiation alone but reduced when the cells were treated with radiation and wortmannin together. Collectively, radiation treatment induced the activation of autophagy and augmented the expression of antiapoptotic proteins, but cotreatment with wortmannin suppressed this elevation in the expression of antiapoptotic proteins in both cell lines (Fig. 2F). In conclusion, these data demonstrated that the elevation of apoptotic molecules was mediated in part by the JAK/STAT transcriptional pathway and in part by induction of the autophagic pathway.

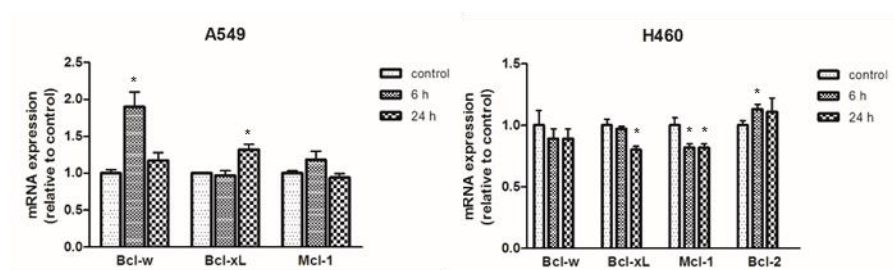


Figure 2A. A549 and H460 cells were irradiated with a dose of 2 Gy, and mRNA expression of antiapoptotic molecules was evaluated by real-time PCR at 6 and 24 hours after irradiation. Asterisks indicate significant differences to control; * $p < 0.05$.

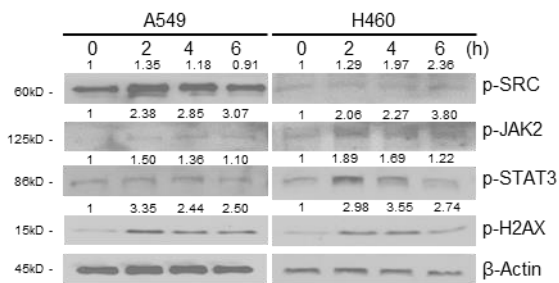


Figure 2B. A549 and H460 cells were irradiated with a dose of 1 Gy, and the phosphorylation of Src, JAK2, and STAT3 was evaluated by immunoblotting at the indicated times after irradiation.

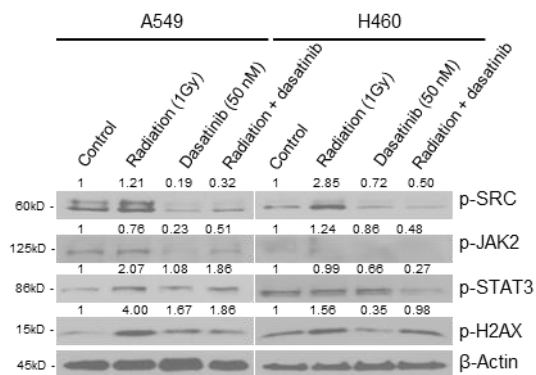


Figure 2C. A549 and H460 cells were exposed to 1 Gy of radiation and/or 50 nM dasatinib for 2 hours. Levels of phospho (p)-Src, p-JAK2, p-STAT3, and p-H2AX (Ser139) were evaluated by immunoblotting 2 hours after treatment. Actin was used as a loading control.

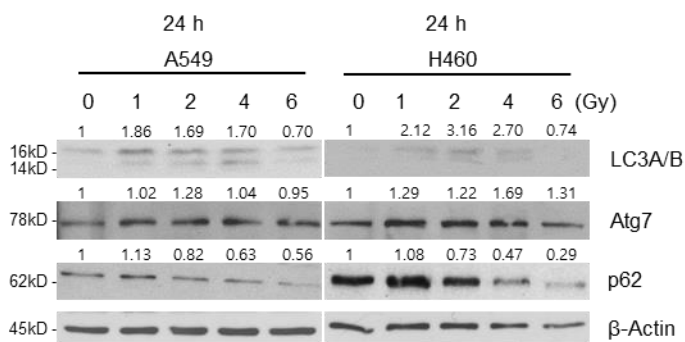


Figure 2D. A549 and H460 cells were irradiated, and the expression of LC3A/B, Atg 7, and p62 was evaluated by immunoblotting 24 hours after irradiation.

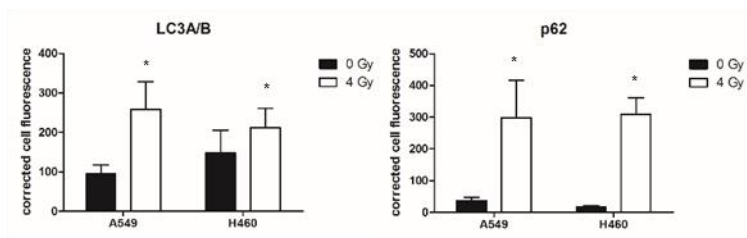
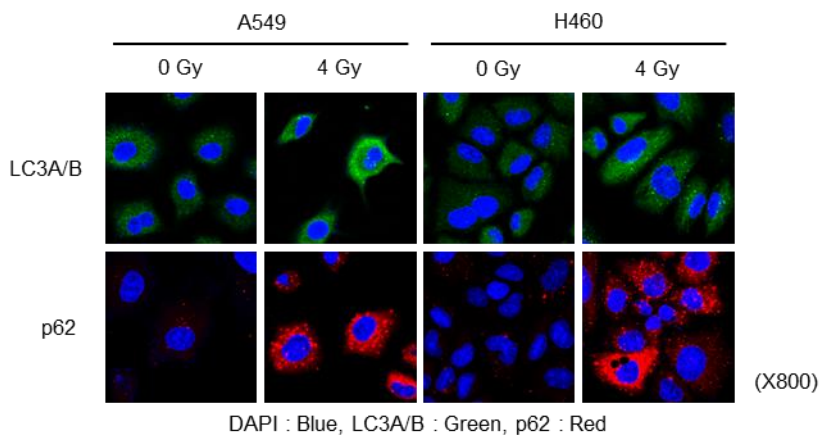


Figure 2E. Confocal microscopy images of A549 and H460 cells after immunofluorescence for LC3A/B (green) and p62 (red) proteins at 24 hours after 4 Gy

of radiation (magnification: 800×). Asterisks indicate significant differences to control;
* $p < 0.05$.

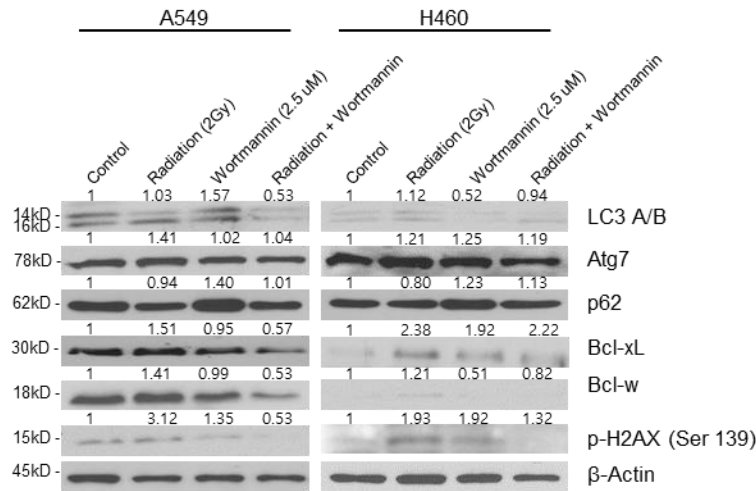


Figure 2F. A549 and H460 cells were exposed to 2 Gy of radiation and/or 2.5 μ M wortmannin for 24 hours. Levels of LC3A/B, Atg 7, p62, p-H2AX (Ser139), and antiapoptotic proteins were evaluated by immunoblotting 24 hours after treatment. Actin was used as a loading control.

3. ABT-737 enhanced the radiosensitivity of A549 and H460 cells

To confirm the radiosensitizing effects of ABT-737, clonogenic assays were performed with A549 and H460 cell lines (Fig. 3A). Cells were treated with 1 μ M ABT-737 or DMSO for 1 h and exposed to 2 Gy of radiation. The number of surviving clones in the combination treatment group was significantly lower than that in the group treated with radiation or ABT-737 alone. In A549 cells, the number of surviving clones in the

combination treatment group was reduced to 32.6% compared to the group treated with either ABT-737 alone (80.4%, $p = 0.001$) or radiation alone (52.2%, $p = 0.021$). In H460 cells, for the combination treatment group, the number of surviving clones was decreased to 9.8% compared with that in the group treated with either ABT-737 alone (75.6%, $p < 0.001$) or radiation alone (30.8%, $p = 0.003$; Fig. 3B). These results indicated that exposure of A549 and H460 cell lines to concurrent treatment with ABT-737 and radiation therapy enhanced the radiosensitivity compared with radiation alone.

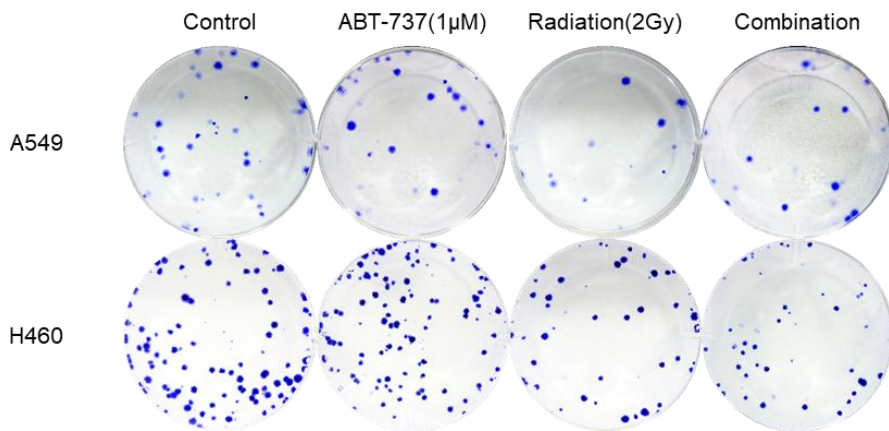


Figure 3A. After treatment with 1 μ M ABT-737 or DMSO for 1 hour, cells were exposed to 2 Gy of radiation, and clonogenic assays were performed.

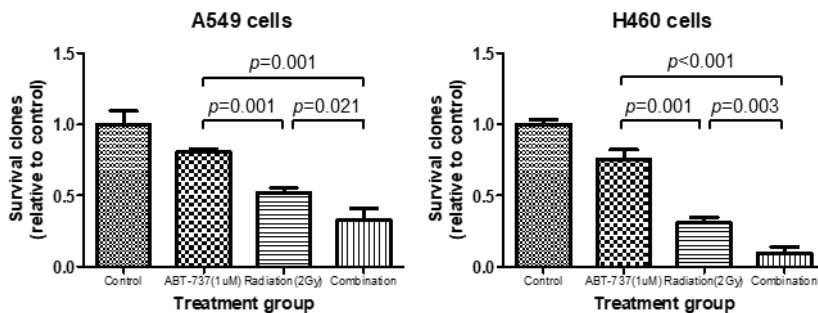


Figure 3B. The number of surviving clones in each group was counted using a cutoff of 50 viable cells.

4. The combination of ABT-737 and irradiation showed increased antitumor efficacy in the Kras^{G12D}:p53^{fl/fl} lung cancer mouse model

To investigate whether ABT-737 could enhance radiosensitizing effects in NSCLC *in vivo*, we used a Kras^{G12D}:p53^{fl/fl} lung cancer mouse model (Fig. 4A). Responses were measured by micro-CT (Fig. 4B). Statistically significant reductions in tumor size were observed in the combination treatment group, in which mice were pretreated with ABT-737 and irradiated ($P = 0.044$; Mann–Whitney U test; Fig. 4C). Lungs were harvested after the second round of micro-CT imaging and analyzed by H&E and IHC (Fig. 4D). In H&E staining, disrupted tumor structures with apoptotic bodies were most frequently observed in the irradiated lungs of ABT-737-pretreated mice. To quantify the apoptotic effects of this combination treatment, IHC analysis of activated caspase-3 was performed. Activated caspase-3 was more abundant in lungs irradiated with ABT-737 pretreatment than in the other groups (Fig. 4E). To determine the effects of combination treatment with ABT-737 and irradiation on survival and toxicity, lung cancer-induced LSL K-ras G12D and p53^{fl/fl} mice pretreated with vehicle or ABT-737 and subjected to irradiation of both lungs were monitored, and their body weights were regularly determined for 80 days after treatment. The median survival times were 95 and 82 days for the vehicle and ABT-737 groups, respectively. Kaplan–Meier survival curves showed that survival was improved in the combination group, although there were no significant differences between the two groups (Fig. 4F). Moreover, body weights in the two groups decreased after approximately 10 days of treatment and thereafter showed a tendency to recover. Body weight changes in the combination group were not significantly different compared with those in the monotherapy group. Thus, these data

suggested that combination treatment with irradiation and ABT-737 caused no obvious systemic toxicity (Fig. 4F).

In summary, we observed significant tumor reduction in lung cancer-induced LSL *K-ras* G12D and p53^{fl/fl} mice following combined treatment with ABT-737 and irradiation compared with vehicle or radiation treatment alone.

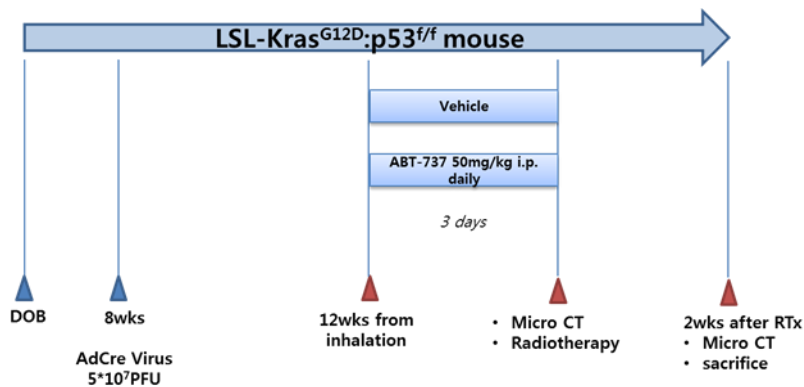


Figure 4A. Treatment schedule for lung cancer-induced LSL *K-ras* G12D and p53^{fl/fl} mice. Eight-week-old heterozygous LSL *K-ras* G12D and p53^{fl/fl} mice were treated with 5×10^7 PFU AdenoCre virus by inhalation. At 12 ± 2 weeks, the mice were randomized and pretreated with either vehicle or ABT-737 for 3 days. Then, mice were irradiated only in the left lung. Micro-CT was performed twice: before irradiation and 2 weeks after irradiation.

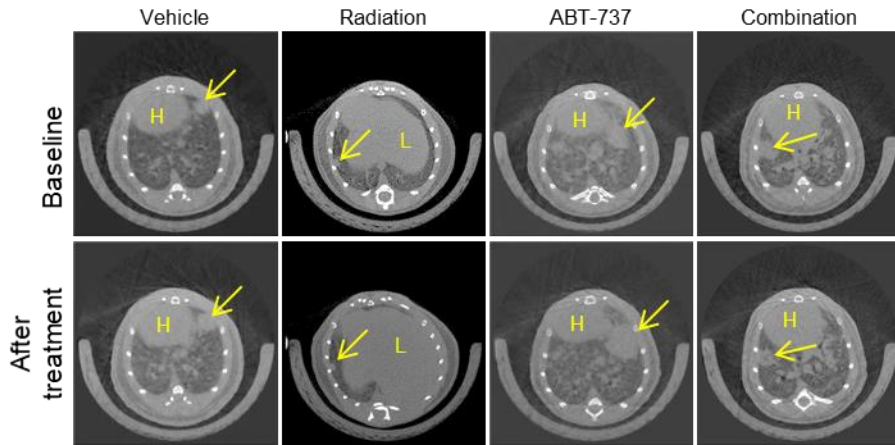


Figure 4B. The treatment response was evaluated by comparing micro-CT images taken before and after treatment. Yellow arrow refers to the representative tumor mass observed in micro-CT images. H; heart, L; liver.

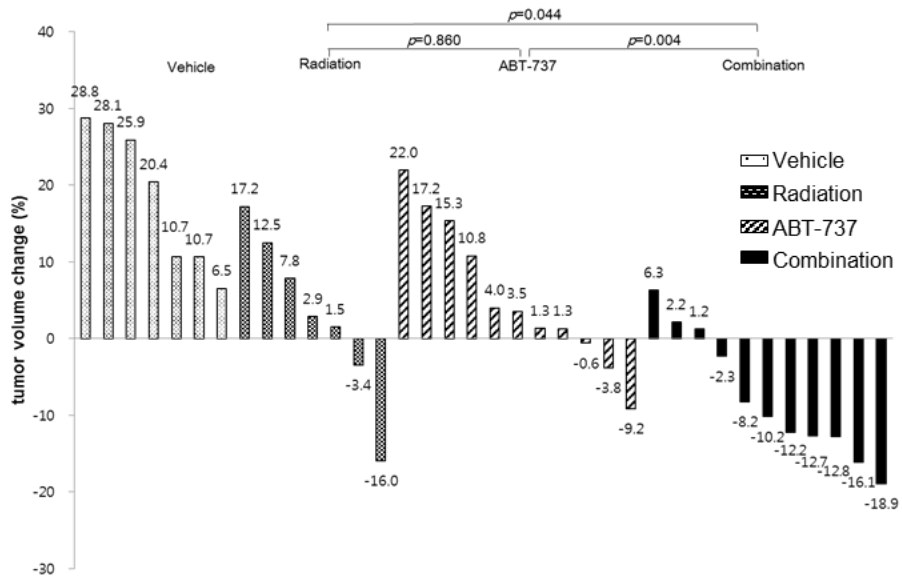


Figure 4C. Waterfall plot showing tumor responses after treatment. Each column represents one individual lung for each mouse. *P* values were obtained by Mann–Whitney U tests.

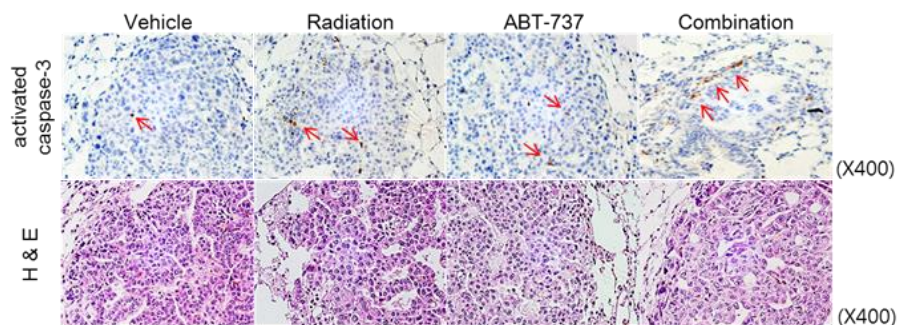


Figure 4D. H&E staining and activated caspase-3 immunohistochemical analysis in the lungs of mice. For immunohistochemistry, DAB was used as a chromogen (magnification: 400×). Positively stained cells with activated caspase-3 are marked with red arrows.

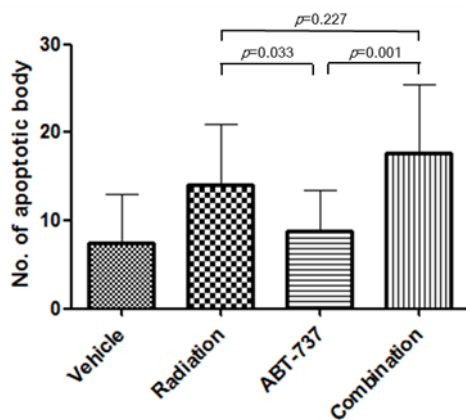


Figure 4E. The number of apoptotic bodies per high-power field (400×) is presented as a histogram; apoptotic bodies were counted in five fields.

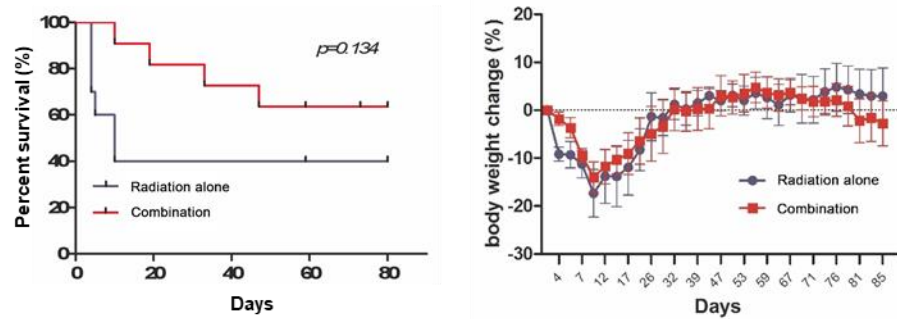


Figure 4F. Effects of combination treatment with ABT-737 and irradiation on overall survival and changes in body weights in mice. Changes in body weights were compared by Mann–Whitney U tests.

IV. DISCUSSION

Overexpression of antiapoptotic Bcl-2 proteins has been observed in a variety of tumor types and is associated with resistance to radiotherapy.¹⁷⁻¹⁹ In this report, we also showed that irradiation induced overexpression of antiapoptotic Bcl-2 proteins. However, the underlying molecular mechanisms of overexpression of antiapoptotic molecules after radiation remain unclear.²⁰

Ho et al. demonstrated that both the RNA and protein levels of Bcl-xL were elevated after irradiation in A549 cells and that radiation enhanced STAT3 phosphorylation.¹⁸ Additionally, Li et al. demonstrated that irradiation activated the phosphorylation of STAT3 and increased the invasion of A549 cells.²¹ In the present study, the mRNA levels of antiapoptotic molecules were augmented in A549 cells. Additionally, the phosphorylation of Src was related to the phosphorylation of STAT3 through JAK2; p-Src, p-JAK2, and p-STAT3 levels were diminished after treatment with the Src inhibitor dasatinib. Overall, our findings demonstrated that the elevation of apoptotic molecules was mediated by the JAK/STAT transcriptional pathway.

Unlike A549 cells, the increase in mRNA expression was not clear in H460 cells. This suggested that mechanisms other than transcriptional regulation may be involved in mediating the expression of antiapoptotic proteins. Autophagy is another factor affecting protein expression at the posttranscriptional level. The expression levels of LC3A/B and Atg7 were augmented after irradiation with increasing doses of radiation up to 2 or 4 Gy and then diminished, similar to the pattern of γ -H2A.X and anti-apoptotic protein expression. This phenomenon might be related to cell viability after radiation. In other words, up to a certain dose of radiation, the expression of the related protein is increased. However, if the radiation dose increased up to the lethal dose, the

cell viability would be decreased significantly, and the protein expression would also be decreased accordingly.

We showed increased LC3-II protein levels together with a slight reduction in p62 protein levels and intense LC3A/B expression by confocal microscopy, indicating increased autophagic flux.²² According to previous studies, irradiation can induce ‘early’ expression of p62 mRNA, and intensification of p62 transcription can lead to overexpression in the context of increased autophagy flux in lung cancer cell lines.^{23,24} We considered that this discrepancy in the blotting and confocal microscopy seems to be due to differences in the timepoint. Additionally, the increased autophagy and expression of antiapoptotic proteins after irradiation were reduced when A549 and H460 cell lines were treated with wortmannin, an autophagy inhibitor. Some studies have shown intensified autophagic flux after radiation treatment in NSCLC cell lines.^{23,25} Jo et al. showed that autophagy appeared earlier than apoptosis after irradiation and that a portion of apoptosis was autophagy-dependent in malignant glioma cells.²⁶ Thus, our findings demonstrated that radiation induced increased expression of autophagy, indicating that the autophagic pathway induced by irradiation was associated with elevation of apoptotic proteins and radioresistance in NSCLC.

Although the mechanisms of cancer radioresistance are complicated and affected by many factors, it is clear that overexpression of antiapoptotic proteins is closely related to the radioresistance of cancer cells.²⁷ Our study showed overexpression of antiapoptotic proteins after irradiation, and targeting these proteins could be a potential method to enhance the effects of irradiation treatment. ABT-737 binds Bcl-2 and Bcl-xL with high affinity, and many Bcl-2 family inhibitors, including ABT-737, show radiosensitizing effects in a variety of tumor types.²⁸⁻³⁰ Additionally, we tried to investigate the molecular mechanism of the radiosensitization effect of ABT-737 by showing the increase of activated caspase-3 and cleaved PARP through immunoblotting. Unfortunately, its expressions were not evident in the cell lines used in these

experiments, so we were unable to investigate the significant relationships of ABT-737 and the radiosensitization effect further. More experiments would be needed to determine exactly how ABT-737 affects radiosensitization.

ABT-737 and ABT-263 (the oral form of ABT-737), as single agents in clinical trials, showed efficacy in hematologic malignancies but demonstrated limited success in solid tumors.^{31,32} Although a few studies have demonstrated the radiosensitizing effects of ABT-737 in some solid tumors, including breast, head and neck, and cervical cancer,^{20,30,33,34} there are few data describing the radiosensitizing effects of ABT-737 in lung cancer as a single agent. Only one study showed the radiosensitizing effect of combination treatment with ABT-737 and a mTOR inhibitor in NSCLC cells;³⁵ however, these effects were only demonstrated in an *in vitro* study and lung cancer xenograft model. The cancer stroma is distinct from the normal stroma and provides a supportive microenvironment for tumor growth; xenografts do not reflect this tumor microenvironment.³⁶ We used genetically engineered mouse models, which mimic the mechanisms of human malignancies and are thought to be more clinically relevant animal models than xenograft models.³⁷ We first evaluated the radiosensitizing effects of ABT-737 using micro-CT image analysis, which enabled quantitative analysis, in a real-time, noninvasive manner. Furthermore, in most studies of the radiosensitizing effects of ABT-737, researchers showed the efficacy of the drug but did not perform an assessment of the toxicity of the drug. In the radiation treatment of mice in our study, body weight changes were not significant between the ABT-737 and control groups. However, additional assessment of drug toxicity is needed. Survival analysis of the mice for 80 days showed that the ABT-737 combination group survived longer than the control group, although a significant difference was not observed between the two groups. In a study of the natural course of LSL *K-ras* G12D and p53^{fl/fl} mouse models using AdCre virus inhalation, the median survival of mice was 76 days.³⁸ In this study, the mice were infected with 2.5×10^7 PFU AdCre virus, which was half the level of our research. Considering that the amount of inhaled virus increased the tumor burden, our

experimental data showed the prolonged survival of mice with a higher tumor burden. That is, radiation therapy or combination treatment might increase the survival of mice compared with nonirradiated, nontreated mice. The lack of a difference between the radiation group and the combination group in our research may be due to the small number of animals or the short observation period. Additional studies are needed to supplement these findings.

Another study reported that selective inhibitors of Bcl-xL, BXI-61 and BXI-72 exhibit more potent efficacy in lung cancer than ABT-737.³⁹ It demonstrated that BXI-72 showed a better anticancer effect than BXI-61 and ABT-737, and BXI-72 showed a radiosensitizing effect in a NSCLC xenograft model. However, our study has its own significant advantage of using GEMM, which could reflect the tumor microenvironment. Additionally, BXI-72 did not show a significant difference from ABT-737 in terms of side effects.

V. CONCLUSION

In conclusion, this preclinical study supported the therapeutic potential of ABT-737 treatment to sensitize lung cancer to radiotherapy. The rational therapeutic targeting of Bcl-2 family proteins by ABT-737 is a potential strategy to overcome possible resistance in K-ras mutant NSCLC to standard radiotherapy. Clinical trials are warranted to determine whether this novel strategy may benefit patients with NSCLC.

REFERENCES

1. Siegel RL, Miller KD, Fuchs HE, Jemal A. Cancer Statistics, 2021. *CA Cancer J Clin* 2021;71:7-33.
2. Lehman M. Improving Therapeutic Outcomes in Non-small Cell Lung Cancer not Suitable for Curative Intent Therapy - A Review of the Role of Radiation Therapy in an Era of Increasing Systemic Therapy Options. *Clin Oncol (R Coll Radiol)* 2016;28:327-33.
3. Impicciatore G, Sancilio S, Miscia S, Di Pietro R. Nutlins and ionizing radiation in cancer therapy. *Curr Pharm Des* 2010;16:1427-42.
4. Bischoff P, Altmeyer A, Dumont F. Radiosensitising agents for the radiotherapy of cancer: advances in traditional and hypoxia targeted radiosensitisers. *Expert Opin Ther Pat* 2009;19:643-62.
5. Galeaz C, Totis C, Bisio A. Radiation Resistance: A Matter of Transcription Factors. *Frontiers in Oncology* 2021;11.
6. Adams JM, Cory S. The Bcl-2 protein family: arbiters of cell survival. *Science* 1998;281:1322-6.
7. Moretti L, Li B, Kim KW, Chen H, Lu B. AT-101, a pan-Bcl-2 inhibitor, leads to radiosensitization of non-small cell lung cancer. *J Thorac Oncol* 2010;5:680-7.
8. Haura EB, Cress WD, Chellappan S, Zheng Z, Bepler G. Antiapoptotic signaling pathways in non-small-cell lung cancer: biology and therapeutic strategies. *Clin Lung Cancer* 2004;6:113-22.
9. Borner MM, Brousset P, Pfanner-Meyer B, Bacchi M, Vonlanthen S, Hotz MA, et al. Expression of apoptosis regulatory proteins of the Bcl-2 family and p53 in primary resected non-small-cell lung cancer. *Br J Cancer* 1999;79:952-8.
10. Mirkovic N, Voehringer DW, Story MD, McConkey DJ, McDonnell TJ, Meyn RE. Resistance to radiation-induced apoptosis in Bcl-2-expressing cells is reversed by depleting cellular thiols. *Oncogene* 1997;15:1461-70.

11. Kyprianou N, King ED, Bradbury D, Rhee JG. bcl-2 over-expression delays radiation-induced apoptosis without affecting the clonogenic survival of human prostate cancer cells. *Int J Cancer* 1997;70:341-8.
12. Baell JB, Huang DC. Prospects for targeting the Bcl-2 family of proteins to develop novel cytotoxic drugs. *Biochem Pharmacol* 2002;64:851-63.
13. Zhang L, Ming L, Yu J. BH3 mimetics to improve cancer therapy; mechanisms and examples. *Drug Resist Updat* 2007;10:207-17.
14. Oltersdorf T, Elmore SW, Shoemaker AR, Armstrong RC, Augeri DJ, Belli BA, et al. An inhibitor of Bcl-2 family proteins induces regression of solid tumours. *Nature* 2005;435:677-81.
15. Lee EF, Czabotar PE, Smith BJ, Deshayes K, Zobel K, Colman PM, et al. Crystal structure of ABT-737 complexed with Bcl-xL: implications for selectivity of antagonists of the Bcl-2 family. *Cell Death Differ* 2007;14:1711-3.
16. Franken NA, Rodermond HM, Stap J, Haveman J, van Bree C. Clonogenic assay of cells in vitro. *Nat Protoc* 2006;1:2315-9.
17. Pietenpol JA, Papadopoulos N, Markowitz S, Willson JK, Kinzler KW, Vogelstein B. Paradoxical inhibition of solid tumor cell growth by bcl2. *Cancer Res* 1994;54:3714-7.
18. Ho JN, Kang GY, Lee SS, Kim J, Bae IH, Hwang SG, et al. Bcl-XL and STAT3 mediate malignant actions of gamma-irradiation in lung cancer cells. *Cancer Sci* 2010;101:1417-23.
19. Lee JU, Hosotani R, Wada M, Doi R, Kosiba T, Fujimoto K, et al. Role of Bcl-2 family proteins (Bax, Bcl-2 and Bcl-X) on cellular susceptibility to radiation in pancreatic cancer cells. *Eur J Cancer* 1999;35:1374-80.
20. Li JY, Li YY, Jin W, Yang Q, Shao ZM, Tian XS. ABT-737 reverses the acquired radioresistance of breast cancer cells by targeting Bcl-2 and Bcl-xL. *J Exp Clin Cancer Res* 2012;31:102.

21. Li F, Gao L, Jiang Q, Wang Z, Dong B, Yan T, et al. Radiation enhances the invasion abilities of pulmonary adenocarcinoma cells via STAT3. *Mol Med Rep* 2013;7:1883-8.
22. Bjorkoy G, Lamark T, Brech A, Outzen H, Perander M, Overvatn A, et al. p62/SQSTM1 forms protein aggregates degraded by autophagy and has a protective effect on huntingtin-induced cell death. *J Cell Biol* 2005;171:603-14.
23. Karagounis IV, Kalamida D, Mitrakas A, Pouliliou S, Liouisia MV, Giatromanolaki A, et al. Repression of the autophagic response sensitises lung cancer cells to radiation and chemotherapy. *Br J Cancer* 2016;115:312-21.
24. Settembre C, Di Malta C, Polito VA, Garcia Arencibia M, Vetrini F, Erdin S, et al. TFEB links autophagy to lysosomal biogenesis. *Science* 2011;332:1429-33.
25. Liu M, Ma S, Liu M, Hou Y, Liang B, Su X, et al. Synergistic killing of lung cancer cells by cisplatin and radiation via autophagy and apoptosis. *Oncol Lett* 2014;7:1903-10.
26. Jo GH, Bogler O, Chwae YJ, Yoo H, Lee SH, Park JB, et al. Radiation-induced autophagy contributes to cell death and induces apoptosis partly in malignant glioma cells. *Cancer Res Treat* 2015;47:221-41.
27. Chang L, Graham P, Hao J, Ni J, Deng J, Bucci J, et al. Cancer stem cells and signaling pathways in radioresistance. *Oncotarget* 2016;7:11002-17.
28. An J, Chervin AS, Nie A, Ducoff HS, Huang Z. Overcoming the radioresistance of prostate cancer cells with a novel Bcl-2 inhibitor. *Oncogene* 2007;26:652-61.
29. Zerp SF, Stoter R, Kuipers G, Yang D, Lippman ME, van Blitterswijk WJ, et al. AT-101, a small molecule inhibitor of anti-apoptotic Bcl-2 family members, activates the SAPK/JNK pathway and enhances radiation-induced apoptosis. *Radiat Oncol* 2009;4:47.
30. Wu H, Schiff DS, Lin Y, Neboori HJ, Goyal S, Feng Z, et al. Ionizing radiation sensitizes breast cancer cells to Bcl-2 inhibitor, ABT-737, through regulating Mcl-1. *Radiat Res* 2014;182:618-25.

31. Roberts AW, Seymour JF, Brown JR, Wierda WG, Kipps TJ, Khaw SL, et al. Substantial susceptibility of chronic lymphocytic leukemia to BCL2 inhibition: results of a phase I study of navitoclax in patients with relapsed or refractory disease. *J Clin Oncol* 2012;30:488-96.
32. Gandhi L, Camidge DR, Ribeiro de Oliveira M, Bonomi P, Gandara D, Khaira D, et al. Phase I study of Navitoclax (ABT-263), a novel Bcl-2 family inhibitor, in patients with small-cell lung cancer and other solid tumors. *J Clin Oncol* 2011;29:909-16.
33. Gilormini M, Malesys C, Armandy E, Manas P, Guy JB, Magne N, et al. Preferential targeting of cancer stem cells in the radiosensitizing effect of ABT-737 on HNSCC. *Oncotarget* 2016;7:16731-44.
34. Wang H, Yang YB, Shen HM, Gu J, Li T, Li XM. ABT-737 induces Bim expression via JNK signaling pathway and its effect on the radiation sensitivity of HeLa cells. *PLoS One* 2012;7:e52483.
35. Kim KW, Moretti L, Mitchell LR, Jung DK, Lu B. Combined Bcl-2/mammalian target of rapamycin inhibition leads to enhanced radiosensitization via induction of apoptosis and autophagy in non-small cell lung tumor xenograft model. *Clin Cancer Res* 2009;15:6096-105.
36. Walrath JC, Hawes JJ, Van Dyke T, Reilly KM. Genetically engineered mouse models in cancer research. *Adv Cancer Res* 2010;106:113-64.
37. Fushiki H, Kanoh-Azuma T, Katoh M, Kawabata K, Jiang J, Tsuchiya N, et al. Quantification of mouse pulmonary cancer models by microcomputed tomography imaging. *Cancer Sci* 2009;100:1544-9.
38. DuPage M, Dooley AL, Jacks T. Conditional mouse lung cancer models using adenoviral or lentiviral delivery of Cre recombinase. *Nat Protoc* 2009;4:1064-72.
39. Park D, Magis AT, Li R, Owonikoko TK, Sica GL, Sun SY, et al. Novel small-molecule inhibitors of Bcl-XL to treat lung cancer. *Cancer Res* 2013;73:5485-96.

ABSTRACT(IN KOREAN)

전리 방사선 치료시 발생하는 항세포 고사 경로 일탈 기전의 극복을
통한 새로운 폐암 치료법 개발

<지도교수 장윤수>

연세대학교 대학원 의학과

이 정 모

종양의 방사선 저항과 선량 제한 독성은 방사선 치료의 치료 잠재력을 제한한다. 따라서 이런 한계를 극복하고 효능을 증가시키기 위한 새로운 접근법이 필요하다. 본 연구에서 우리는 방사선 조사를 통해 얻어진 autophagy의 유도 및 STAT3 활성화가 항고사 단백 (anti-apoptotic proteins)에 미치는 영향을 확인하였다. 또한 K-ras 돌연변이 비소세포 폐암 세포 및 Kras^{G12D}:p53^{fl/fl} 쥐 모델을 사용하여 BH3 모방체인 ABT-737의 방사선 증감제 (radiosensitizer)로서의 효과를 확인하였다.

먼저, A549 및 H460 세포에 방사선을 조사하여, Bcl-2 계열 단백질의 발현, JAK/STAT 전사 경로 및 autophagy 경로를 면역 블로팅법을 이용하여 평가하였다. 또한, ABT-737의 방사선 증감 효과는 A549 및 H460 세포주에서 클로노제닉 어세이(clonogenic assay)를 이용하여 평가하였고, Kras^{G12D}:p53^{fl/fl} 쥐 모델에서 마이크로 전산화 단층촬영 및 면역화학염색을 이용하여 평가

했다.

방사선 조사는 A549 및 H460 세포와 마우스 폐 조직에서 Bcl-xL, Bcl-2, Bcl-w 및 Mcl-1 등의 항고사 단백질의 과발현을 유도하였다. 이런 Bcl-2 계열 단백질의 과발현은 방사선에 의한 Janus kinase/STAT 전사 신호 장애 및 autophagy 경로의 활성화를 통해 유도 되었다. A549 및 H460 세포주를 ABT-737로 처리한 후 방사선 피폭시, 병합 치료 그룹의 생존 클론의 수는 방사선을 단독으로 처리한 그룹 또는 ABT-737단독으로 처리한 그룹보다 현저히 낮았다. KP 마우스 폐암 모델에서도 방사선 조사와 ABT-737의 병합 치료는 단독 치료군들 대비 현저한 폐암의 감소를 유도했다. 하지만 병합 치료 그룹의 체중 변화는 단독 치료군들 대비 유의미한 차이를 보이지 않았다. 이는 방사선 및 ABT-737 병합 치료가 단독 치료 대비 전신 독성을 유발하지 않았음을 시사한다.

이러한 연구결과는 전임상 모델에서 ABT-737의 방사선 증감제로서의 역할을 지지했으며, 이 전략을 사용한 임상 실험이 K-ras 돌연변이 비소세포 폐암에 도움이 될 수 있음을 시사한다.

핵심되는 말 : 비소세포폐암, 세포 고사, 방사선 증감제, ABT-737